

Energy harvesting from asphalt pavement using thermoelectric technology

Wei Jiang ^{a,*}, Dongdong Yuan ^a, Shudong Xu^a, Huitao Hu^a,

Jingjing Xiao ^b, Aimin Sha ^a, Yue Huang ^c

^a Key Laboratory for Special Area Highway Engineering of Ministry of Education, Chang'an University, South 2nd ring road Middle Section, Xi'an, Shaanxi, 710064, China

^b School of Civil Engineering, Chang'an University, South 2nd ring road Middle Section, Xi'an, Shaanxi, 710064, China

^c Department of Civil Engineering, Liverpool John Moores University, Peter Jost Enterprise Centre, Byrom Street, L3 3AF Liverpool, United Kingdom

* Corresponding author. *E-mail address*: jiangwei_029@sina.com (W. Jiang).

Abstract: Nowadays, energy harvesting from road has become a research hotspot. The power generation system within asphalt pavement based on thermoelectric technology was studied in this paper. The characteristics of temperature difference between the pavement and ambient air, as well as the temperature gradient within road surface were investigated by collecting data on-site in different seasons. Based on this, a novel set of road thermoelectric generator system (RTEGS) was developed, which can generate electricity when there is a temperature difference between road surface and ambient air. In addition, a RTEGS prototype was fabricated to verify the energy generation capacity based on indoor and outdoor tests. Results showed that the output voltage of RTEGS was about 0.4 V by asphalt mixture slab (300 mm × 300 mm by size), when the temperature difference between road surface and ambient air was 15 °C in winter. While in summer, the output voltage was about 0.6 V to 0.7 V, with a temperature difference of 25 °C to 30 °C. This means that some 160 kWh of energy can be obtained in 8 hours from a road of 1 km in length and 10 m in width. For asphalt pavement in tropical and subtropical regions, the large temperature difference would be more suitable for RTEGS. The findings and research experiments from this study will provide a good starting point and reference for the development and application of pavement thermoelectric technology.

Key words: Thermoelectric generator, Energy harvesting, Asphalt pavement, Temperature gradient

1. Introduction

Global energy shortage, environmental pollution and climate change are the most urgent challenges mankind have ever faced [1,2]. The hope of future energy security lies in the economical, efficient and clean use of existing energy, as well as development of new energy sources [3-6]. To this end, environmentally friendly collection and use of clean energy have been explored by industries from different perspectives [7,8]. In pavement engineering, energy harvesting technology becomes a focal point of interdisciplinary research [9-12].

By far, research on energy harvesting from road pavement has focused on the following 3 aspects. 1) Piezoelectric technology. By embedding piezoelectric materials in the pavement structure, a portion of the mechanical energy generated from tyre-road interactions can be converted into electric energy [13-16]. 2) Photovoltaic technology. Using solar panels to replace traditional asphalt and concrete materials on paved roads, which will absorb the solar radiation and transform it into electric energy [17,18]. 3) Thermoelectric technology. By laying thermoelectric generators (TEGs) inside or outside the pavement structure, part of the thermal energy absorbed by the road surface can be converted into electric energy. At this stage, these different ways of pavement energy harvesting have not seen wide range of applications mainly due to technical challenges. Regarding pavement piezoelectric technology, the difficulties include poor durability of piezoelectric materials under repeated traffic loading, the mismatch in stiffness of piezoelectric materials and pavement materials, and the difficulty in directly using the instantaneous high-voltage, low-current electrical signals [14,19]. For pavement photovoltaic

technology, the main difficulties are the need to develop new solar panels that meet the requirements for use in road surface. Durability of the photovoltaic power generation system influenced by external factors such as traffic load, rain and snow, etc. is crucial to prevent efficiency loss of the solar panels, and to meet requirements such as driving comfort, skid-resistance, and easy-to-repair [20] etc. As to pavement thermoelectric technology, the challenges mainly lie in the low efficiency of power generation which relies on the temperature gradients within pavement structures [21].

Compared with piezoelectric and photoelectric modes, pavement thermoelectric technology has its own superiorities despite of the currently low efficiency. The thermal energy absorbed by road surface can be directly converted into electric energy without changing pavement materials and structures. On the one hand, the heat transition can reduce plastic deformation caused by rising temperature within asphalt pavement in hot weather, and thus prolong the service life of road [22]. On the other hand, through the diversion of heat from road surface, the urban heat island effect which is caused by the heat absorption and storage inside the asphalt pavement, can be mitigated [23-25].

TEG produces electric energy based on the Seebeck effect [26], i.e. the voltage output is caused by temperature difference between the two (hot and cold) sides of TEG. The fundamental principle is based on the charge carriers: electrons in N-type materials and holes in P-type materials have the ability to move freely through metals and semiconductors [27]. In the presence of a temperature gradient, charge carriers diffuse from hot side to cold side until an equilibrium is reached between the diffusion potential and the electrostatic repulsion potential, resulting in a buildup of charge carriers [28]. Typical thermoelectric devices consist of alternating P and N-type

semiconductors connected electrically in series and thermally in parallel as shown in Fig. 1. This allows the holes and electrons to flow in opposite directions forming an electric current for power generation.

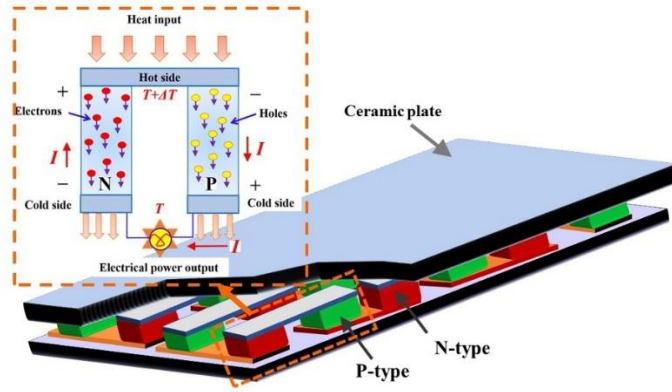


Fig. 1. Configuration of TEG module.

The temperature difference determines the efficiency of power generation in TEGs. The greater the temperature gradient, the more energy is generated. The temperature difference can be found from pavement materials at different depths. However, this difference is limited due to the small temperature gradient within the pavement structure [29,30]. Wu et al. (2011) developed devices made of highly thermal-conductive materials to exploit the temperature difference between the subgrade and road surface which facilitated the electricity generation [31,32]. Hasebe et al. (2006) developed a pavement-cooling system (water pipes) with a TEG embedded in the pavement [33]. River water near the road was used as a coolant to collect heat from the hot side of TEG and provide heat for the cold side. A similar pipe-pavement TEG system model was developed by Guo L et al. [34], in which the electric energy output was estimated using results from previous studies as well as weather data in Florida, USA. The pavement thermoelectric technology has not yet been comprehensively investigated, due to the low efficiency of power generation caused by low temperature gradients within pavement structures.

In summary, the main challenges of pavement thermoelectric technology are effectively using the temperature difference within road structures, as well as maintaining pavement thermoelectric conversion efficiency under different environmental conditions. Researches so far have been limited to theoretical modelling and estimation, and there is generally a lack of field data to validate the modelling results [35]. In this paper, the road temperature gradients in different seasons were measured and characterized. Then, a novel set of road thermoelectric generator system (RTEGS) was developed. Furthermore, the electrical outputs of RTEGS were tested indoor and outdoor. The voltage and quantity generated by RTEGS were analyzed under different environmental conditions. Findings from this study will provide a starting point and reference for the development and application of pavement thermoelectric technology.

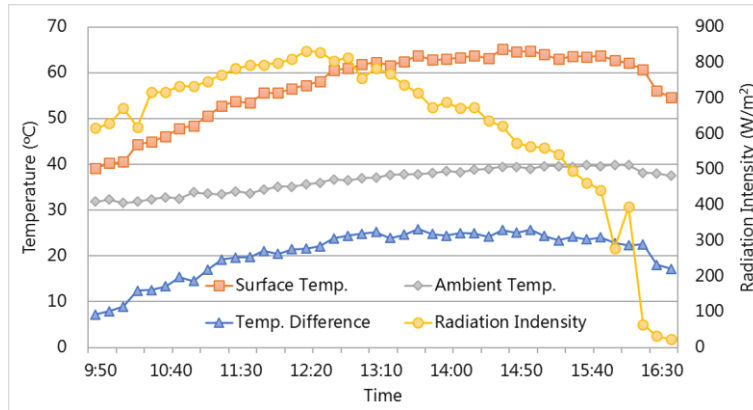
2. Road surface temperature characteristics - preliminary field test

2.1. Temperature difference between road surface and ambient air

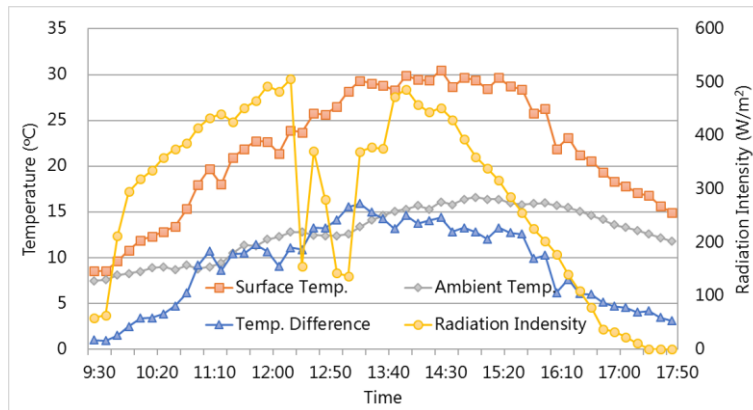
The key to improve the efficiency of RTEGS is to maintain and effectively use the temperature difference. Therefore, it is necessary to examine and analyze the temperature characteristics of road surface and ambient air.

The temperature difference between road surface and ambient air changes due to external circumstances such as radiation intensity. Fig. 2 displays the temperature difference in 7 hours of a typical summer (August 16th, 2016, Fig. 2a) and winter (December 8th, 2016, Fig. 2b) day in the city of Xi'an, China. The temperature of road surface was collected by an infrared thermal imaging camera; the temperature of ambient air and radiation intensity were gathered from a mobile weather station (Fig. 3). Occasional fluctuation of the radiation intensity was observed which was caused by the clouds as well as the moving shadows of surrounding buildings, such

as between 12:00 and 14:00 in Fig. 2b.



(a) August 16th, 2016



(b) December 8th, 2016

Fig. 2. Road surface and ambient air temperature.

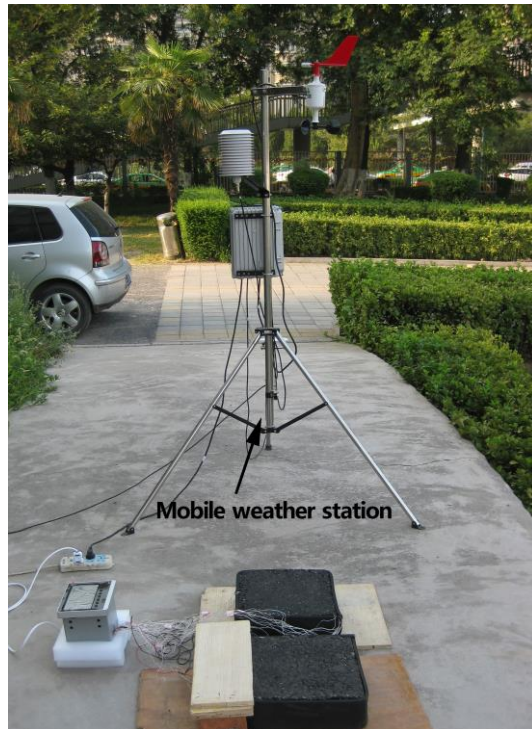


Fig. 3. Mobile weather station device.

It can be seen from Fig. 2 that seasonal variations of radiation intensity have a significant effect on the temperature difference between road surface and ambient air.

On August 16th, 2016, the ambient air temperature was 25 °C to 39 °C, and the solar radiation intensity reached peak value of 833W/m² at 12:30pm. The maximum temperature of road surface was 65 °C, and the temperature difference between road surface and ambient air was up to 25°C. The temperature difference was above 10 °C for 7 h to 8 h, and above 20 °C for about 5 h. On December 8th, 2016, the ambient air temperature was 1 °C to 16 °C, and the solar radiation intensity peak was 506W/m² at 12:30pm. Although the intensity of solar radiation is less in the winter, the road surface temperature reached 30 °C due to the endothermic (heat absorption) effect of asphalt pavement, and the temperature difference between road surface and ambient air was up to 15°C. There were about 5 h when the temperature difference was above 10 °C. Thus, it can be concluded that the temperature differences between road surface and the ambient air always exist for a significant amount of time in the day, regardless of the season.

It is worth noting that the climate of the testing site, located at 33°42' to 34°45' north latitude and 107°40' to 109°49' east longitude, is in the temperate climate zone. It can be predicted that, asphalt pavement in tropical and subtropical regions would be more suitable for the application of pavement thermoelectric technology, for the higher radiation intensity and longer duration of temperature difference.

2.2. Temperature gradient within road pavement

Compared to directly using the temperature difference between road surface and the ambient air, the heat built up inside the road may be easier to use when high efficiency in conduction is achieved via new technology. Therefore, it is useful to determine the temperature gradient

underneath the road surface. Previous work has focused largely on the temperature gradient for the full depth of road [36,37]. However, the temperature gradient within road surface layer, especially the depth from 0 mm to 100 mm, is more valuable for pavement thermoelectric generation technology due to the presence of greater and longer temperature difference [38,39].

In order to obtain accurate data of road surface temperature, asphalt mixture specimen with dimensions of 300 mm \times 300 mm \times 100 mm was prepared in molds. The maximum aggregate size was 9.5mm. The slab was divided into 10 layers, each layer was paved and compacted separately. Two PT100 temperature sensors with 30 mm horizontal spacing were embedded at interfaces between layers. Therefore, a total of 18 temperature sensors were placed in the specimen, as shown in Fig. 4a. The temperatures of slab surface were measured by an infrared thermal imaging camera, and temperature measured by the sensors were collected by a data acquisition instrument. The average temperature of sensors at all interfaces and the temperature obtained from the infrared thermal imaging camera were shown in Fig. 5.

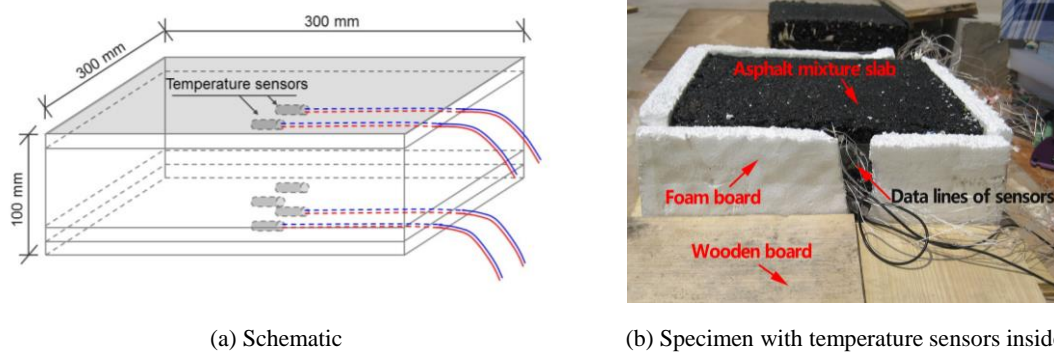
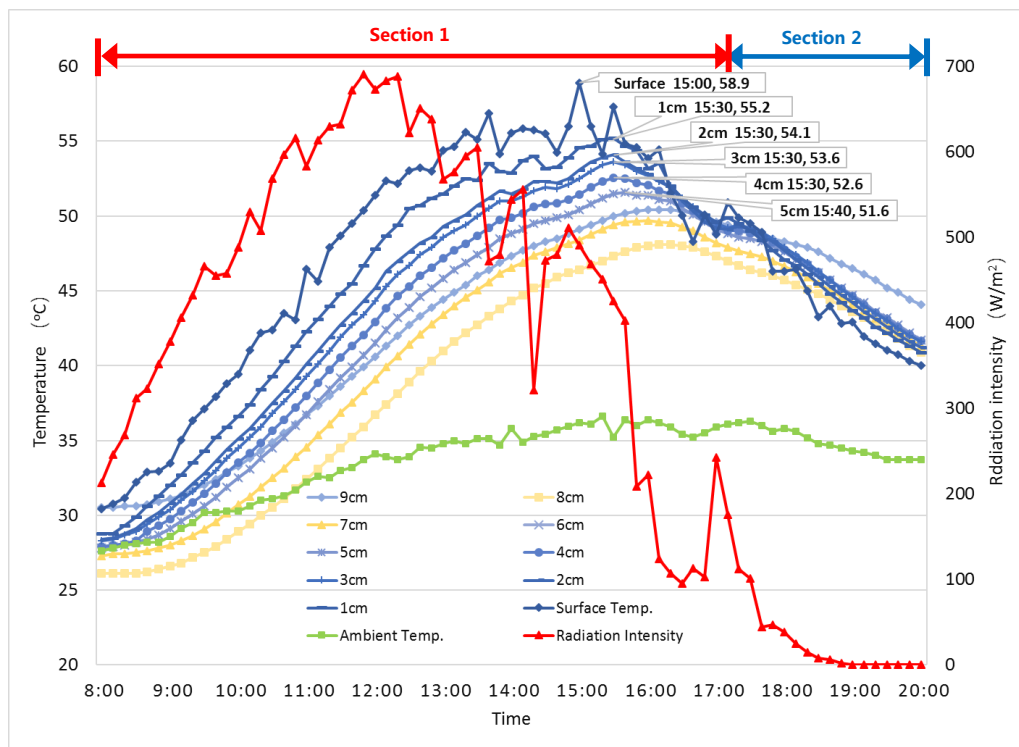


Fig. 4. Placement of temperature sensor in the slab specimen.

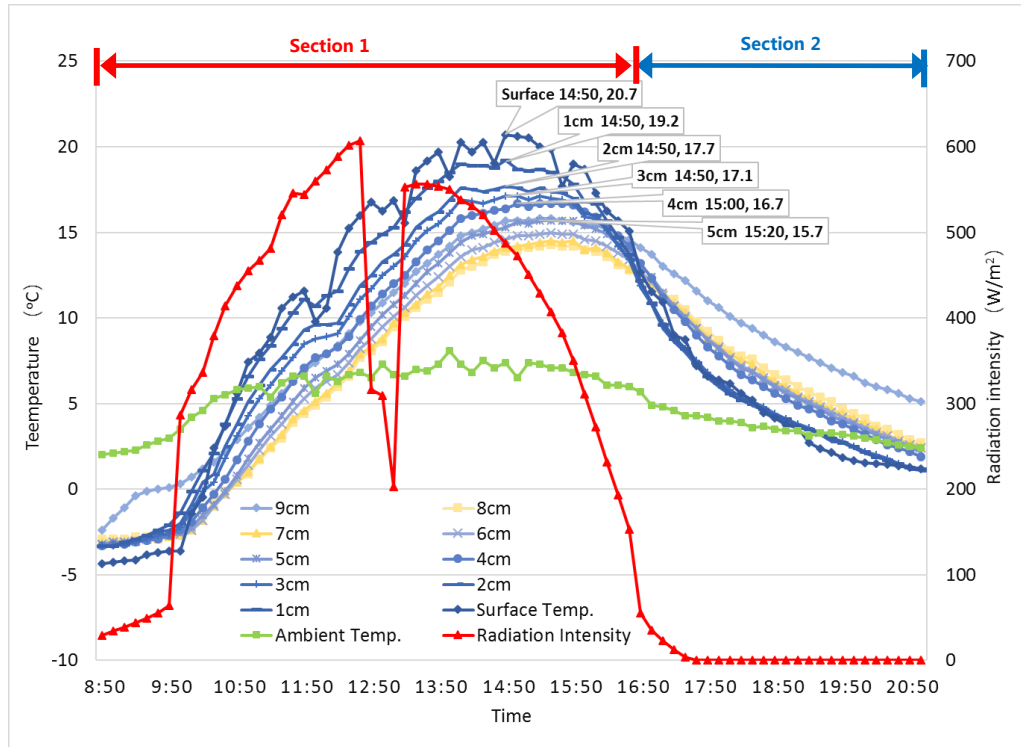
The specimen was placed in a location where it can be exposed to direct sunlight. During the test, the slab was contained in foam boards at all sides and segregated from the concrete floor by a wooden board to reduce external heat transfer, as shown in Fig. 4b.

Fig. 5 gives the temperature data of asphalt mixture slab gathered on August 23rd (Fig. 5a)

and December 27th (Fig. 5b), 2016. It can be seen that, the temperature gradient can be roughly divided into two time sections. In section 1, temperature gradually decreased with the depth due to the amount of solar radiation absorbed by asphalt mixture. When the solar radiation intensity decreased to a certain extent (e.g. below 300 W/m²), the heat absorbed by asphalt pavement materials, especially in surface layers, began to escape into outside, which led to the temperature of road surface being less than lower layers, and this was characterized as section 2.



(a) August 23rd, 2016.



(b) December 27th, 2016.

Fig. 5. Temperature gradient of the asphalt mixture slab.

Surface layer of the road receives solar radiation directly, which is sensitive to the change of radiation intensity. This explains the temperature fluctuation is gradually weakened with the depth. On August 23rd, 2016, the peak value of the slab surface (0 mm depth) temperature was 58.9 °C at 15:00, and the maximum temperature of the slab at 20 mm to 30 mm depth was 55.2 °C at 15:30, i.e. 30 min after the peak temperature at surface. On December 27th, 2016, the peak value of the slab surface temperature was 20.7 °C at 14:50, and the maximum temperature at 20 mm to 30 mm depth was observed at the same time, at 17.1 °C.

The above results show that, although the peak temperature at 20 mm to 30 mm depth was about 3 °C to 4 °C lower than slab surface, it can still maintain a considerable temperature difference to the ambient air. Meanwhile, pavement temperature at this depth varied to a less extent with a change of the solar radiation intensity compared with surface. Therefore, road pavement at 20 mm to 30 mm depth is ideal for experimental thermoelectric generation.

3. Design of road thermoelectric generator system (RTEGS)

The keys principles of RTEGS design include the following. Firstly, to collect and store heat energy from the road surface efficiently. Secondly, to make effective use of the temperature difference between road and ambient air. Thirdly, to minimize the impact of thermoelectric generator system on road structure and material properties.

The RTEGS was designed following the above principles. Vapor chambers, with good heat transfer ability, were placed at 20 mm to 30 mm depth of the road. One end of the vapor chamber was embedded in the pavement structure. The other end was exposed to the roadside and bonded to the hot side of TEG (on its upper surface). The heat collected from the road surface was transferred through the vapor chamber to the hot side of TEG, which formed a temperature difference with the cold side exposed to the environment, thereby generating a voltage, as shown in Fig. 6.

However, the heat would inevitably transfer from TEG hot side to cold side. Therefore, the temperature difference between the TEG and ambient air would eventually diminish to zero. To maintain the temperature difference between the two sides of TEG, a water tank was devised at the TEG cold side as the cooling unit. The bottom of the water tank is a vapor chamber, which is in direct contact with TEG cold side. The sidewalls of the water tank are heat sinks, which enable sufficient heat exchange between the water and ambient air, in order to keep the same temperature. Other measures, such as installing shading board on the outside of the tank to reduce direct sunlight, were also used to reduce the water temperature in the tank.

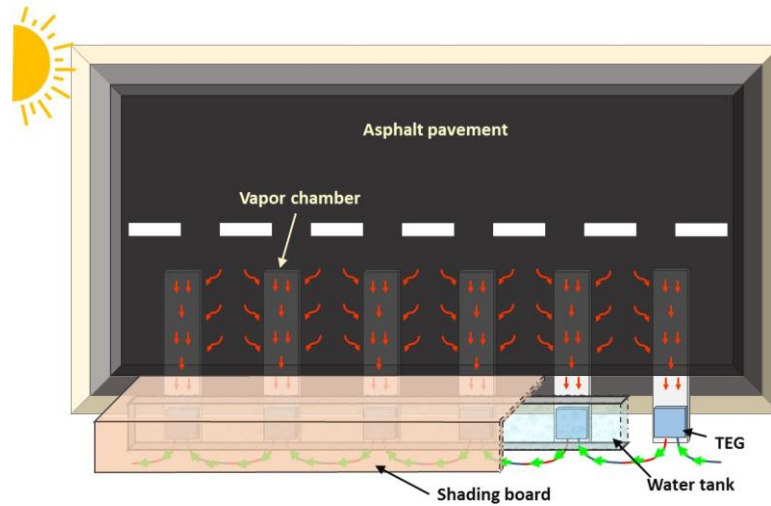


Fig. 6. Schematic of RTEGS.

In this system, the heat was transferred out of the road structure before utilization. Compared with embedding TEGs into the pavement, this system avoids the long-term effects of traffic load on the TEGs, and greatly improves the stability and durability of the RTEGS. Meanwhile, the specially designed water tank makes full use of the temperature difference between the road and ambient air, which enhances the output of electric energy.

4. Materials and test methods of road thermoelectric generator system (RTEGS)

4.1. Materials

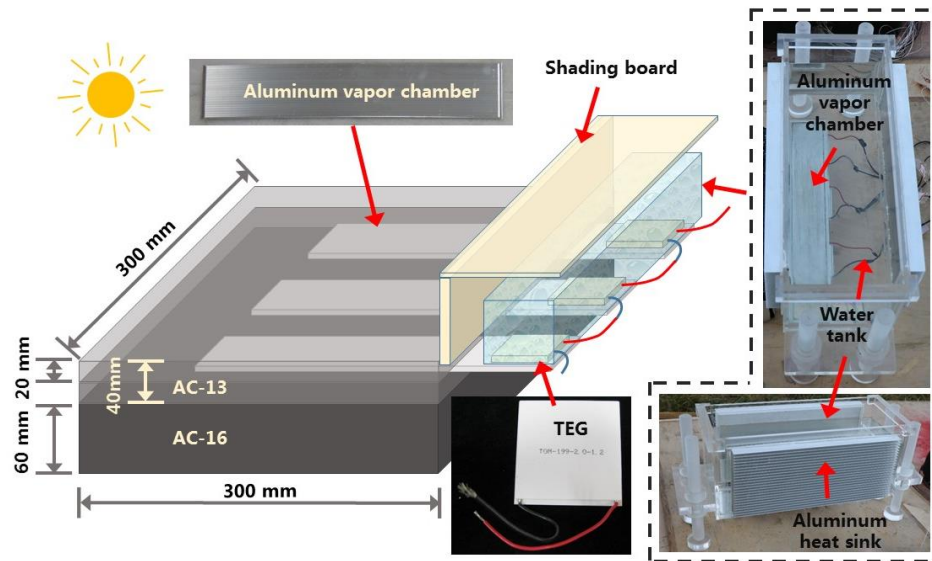
In this study, a RTEGS prototype was developed to verify the ability of the RTEGS to generate electric power in field-simulated roadway conditions. The prototype's components included asphalt mixture slab, power generation device and cooling device for the cold side of TEG, as seen in Fig. 7a.

The asphalt mixture slabs are dual-layer with 300 mm in length, 300 mm in width and 100 mm in thickness. The upper layer is made of SBS modified asphalt mixture with a nominal maximum aggregate size (NMAS) of 13mm, and a layer thickness of 40 mm. The lower layer material is unmodified asphalt mixture with a NMAS of 20 mm and layer thickness of 60 mm.

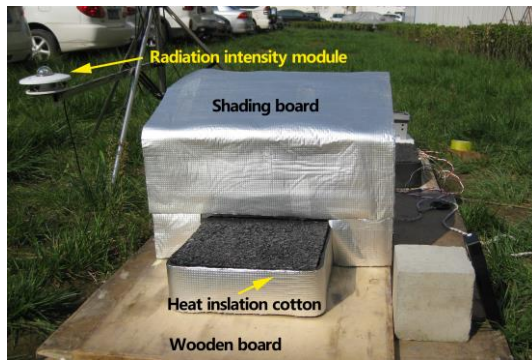
The materials and thickness of the slab are typically found in real road design. In order to reduce the heat exchange between the two sides of the specimen and outside, the slab was surrounded by heat insulation cotton foam and segregated from the ground by a wooden board (Fig. 7b).

The power generation device comprises of aluminum vapor chambers and TEGs. Three pieces of aluminum vapor chambers with $300\text{ mm} \times 60\text{ mm} \times 3\text{ mm}$ dimension were evenly spaced in the slab at 20 mm depth. At one end, about two-thirds of the length was embedded within the slab. At the other end, about 100 mm length was exposed to the outside of the slab, and bonded to the hot side of TEG on the upper surface by thermal adhesive glue. Three TEGs (TEG-199) with 62 mm in length, 62 mm in width and 4 mm in height were connected in series. The TEG-199 module consisted of 199 pairs of semiconductors connected electrically in series and between the hot and cold sides. The equivalent thermal conductivity of the chambers is $3.2 \times 10^6\text{ W/(m}\cdot\text{k)}$, its applicable temperature range is -120°C to 200°C , and its compressive strength is 4 MPa.

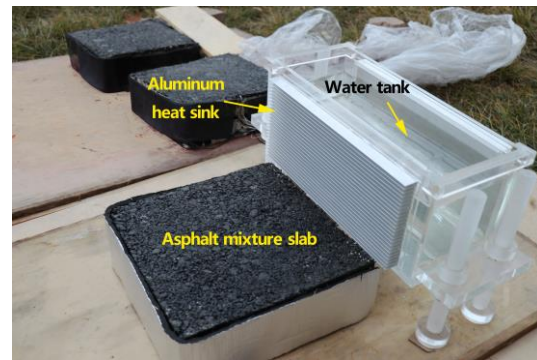
The cooling device includes a shading board and a water tank, which maintains the low temperature at TEG cold side. The water tank with 350 mm (length) \times 150 mm (width) \times 160 mm (height) size is made of polymethyl methacrylate (Fig. 7c). In order to improve the efficiency of heat exchange between TEG cold side and the water in the tank, an aluminum vapor chamber was used at the bottom of the water tank, which is bonded to the TEG cold side by thermal adhesive glue (Fig. 7d and 7f). The sidewalls of water tank are aluminum heat sinks which allowed sufficient heat exchange between the water and ambient air. In addition, the shading boards were used at the side and top of the tank to block direct sunlight.



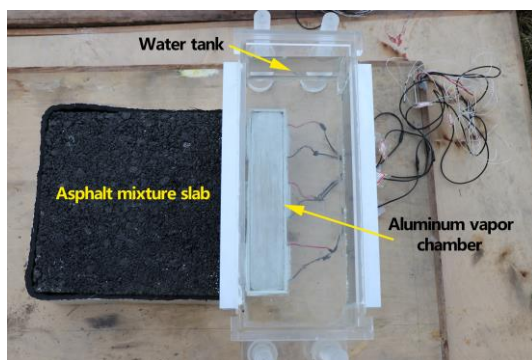
(a) Schematic of RTEGS



(b) Integrated model



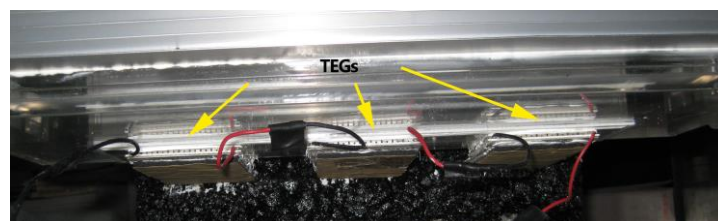
(c) Asphalt mixture slabs and water tank



(d) Details of water tank



(e) Data acquisition instrument



(f) TEGs below the water tank

Fig. 7. Prototype of RTEGS for testing.

4.2. Test methods

4.2.1. Indoor tests

A 500-Watt iodine-tungsten lamp was used to simulate the solar radiation and heat the slab specimens. The perpendicular distance between the slab surface and iodine-tungsten lamp tube was 500 mm. The temperature of slab surface could reach a maximum of 65 °C under the radiation of iodine-tungsten lamp. During the test, Infrared Thermal Imaging Camera was used to record the temperature of slab surface every 10 min, PT100 temperature sensors were used to record the temperature of water in the tank, and the generated electric voltage was gathered by a data acquisition instrument (Fig. 7e).

The environmental conditions can be easily controlled for indoor test. Therefore, it is easy to determine the power generation efficiency of RTEGS under different temperatures and difference conditions. The test methods proposed by the indoor test also provide a reference for subsequent and similar tests.

4.2.2. Outdoor tests

The outdoor tests were considered more representative of the actual generation of electric power by RTEGS because the specimens were put in a natural environment under natural radiation intensity, ambient temperature and other factors such as wind. In the outdoor electric power generation test, the slabs were placed in an open area in order to receive direct sunlight. The data acquisition method was similar to that of indoor tests.

5. Results

5.1. Output voltage of indoor tests

According to the results from indoor tests, linear relationships between temperature

difference and output voltage of RTEGS can be obtained by regression, as shown in Fig. 8. It can be seen that different mathematical relationships between output voltage and temperature difference occurred in the process of heating and cooling. This is because the temperatures of water and TEG cold side are similar, while the temperatures of slab surface and TEG hot side are different. The slab surface temperature was higher than the TEG hot side in the process of heating, and lower than the TEG hot side in the process of cooling. As a result, linear but different relationships exist between the output voltage and temperature difference in the process of slab heating and cooling, the intercepts of the regression lines are different.

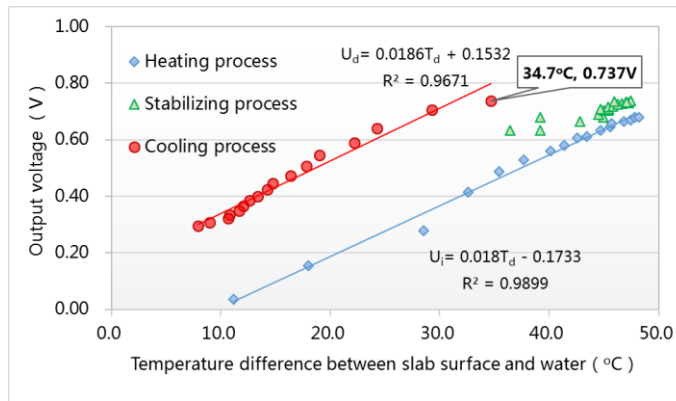


Fig. 8. Relationship between temperature difference and output voltage of RTEGS by indoor test.

The output voltage (U_i) in the process of indoor slab heating can be expressed using the following equation:

$$U_i = 0.018T_d - 0.1733 \quad (R^2 = 0.9899) \quad (1)$$

The output voltage (U_d) in the process of indoor slab cooling can be expressed using the following equation:

$$U_d = 0.0186T_d + 0.1532 \quad (R^2 = 0.9671) \quad (2)$$

where T_d is the temperature difference between the slab surface and water in the tank.

As depicted in Fig. 8, the peak value of output voltage occurred at the initial stage of slab cooling which was 0.737 V, when the temperature difference between the slab surface and water in

the tank was 34.7 °C.

5.2. Output voltage of outdoor tests

Outdoor testing site was selected in Chang'an University, Xi'an on October 31st, 2016. The ambient temperatures of the day were 6 °C to 16 °C. Fig. 9 presents the measured output voltage and temperature data. It can be seen that, the slab surface temperature increased firstly and then began to decline during the test, and the maximum temperature was 36.2 °C. Similar trend can be found for the output voltage. The peak value of output voltage was about 0.41 V. The time that output voltage was above 0.2 V, 0.3 V and 0.4 V was about 6 h, 4 h and 1 h, respectively.

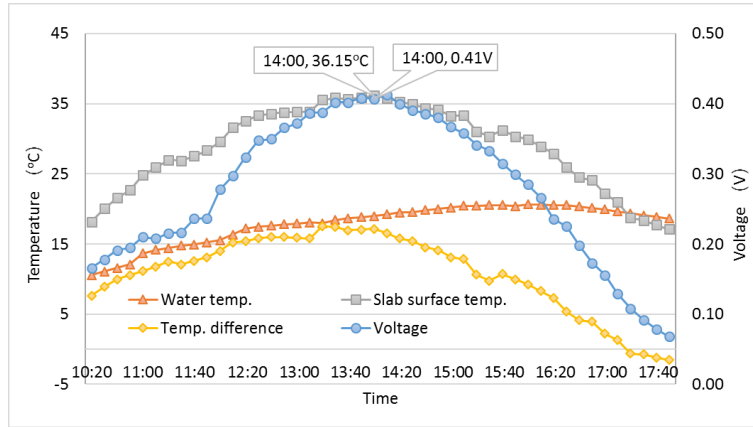


Fig. 9. Output voltage and temperature of RTEGS.

According to the results obtained from outdoor tests, linear relationships between temperature difference (between the slab surface and water in the tank) and output voltage of RTEGS can also be obtained by regression, as shown in Fig. 10. It can be seen that the variations of output voltage with temperature were similar to the results of indoor tests. Good linear correlations between output voltage and temperature difference were observed in the process of slab heating and cooling.

The output voltage (U_i) in the process of outdoor slab heating can be expressed using the following equation:

$$U_i = 0.0204T_d - 0.0100 \quad (R^2 = 0.8904) \quad (3)$$

The output voltage (U_d) in the process of outdoor slab cooling can be expressed using the following equation:

$$U_d = 0.0189T_d + 0.1133 \quad (R^2 = 0.9762) \quad (4)$$

where T_d is the temperature difference between the slab surface and water in the tank.

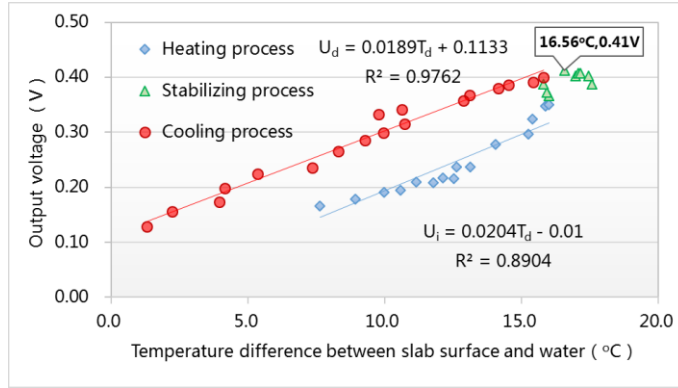


Fig. 10. Relationship between temperature difference and output voltage of RTEGS by outdoor test.

6. Data analysis and discussion

According to the above results, there are some differences in the regression function between indoor and outdoor test. The reason can be attributed to the fact that radiation intensity was gradually changing during the outdoor testing, while it was constant during the indoor testing. As a result, compared with the indoor test, the overall heating rate of the specimen was relatively slow in outdoor test, and the surface and internal temperatures of the specimen were relatively uniform. This difference in radiation intensity led to a difference in the slab temperature gradient, which resulted in a difference in temperature between slab surface and TEG hot side, which is reflected in the regression function eventually.

From the results of outdoor test, there was about 0.4 V output voltage gained from RTEGS when the temperature difference between slab surface and water in the tank was 15 °C. According to the regression relationship between voltage and temperature difference, as well as the road surface temperature gradient, it can be predicted that about 0.6 V to 0.7 V output voltage will be

gained when the road surface temperature reaches 60 °C and the temperature difference between slab surface and water is 25 °C to 30 °C.

The resistance (R) of TEG used in the test is about 1.25 Ω at 20 °C to 60 °C. Therefore, the current and power (P) of the RTEGS can be calculated using Ohm's Law. For example, the output voltage (U) was 0.17 V measured at 10:20am on October 31st, 2016, then the current can be calculated using the following equation.

$$I = \frac{U}{R \times n} = \frac{0.17}{1.25 \times 3} = 0.044 \text{ A} \quad (5)$$

where I is the current (A); n is the number of thermoelectric modules in series and equals to 3 herein;

The power (P) values can be calculated using the following equation.

$$P = UI = 0.17 \times 0.044 = 0.0073 \text{ W} \quad (6)$$

Where P is the power (W);

The power at different times can be calculated based on the output voltage data measured on October 31st, 2016, as shown in Fig. 11.

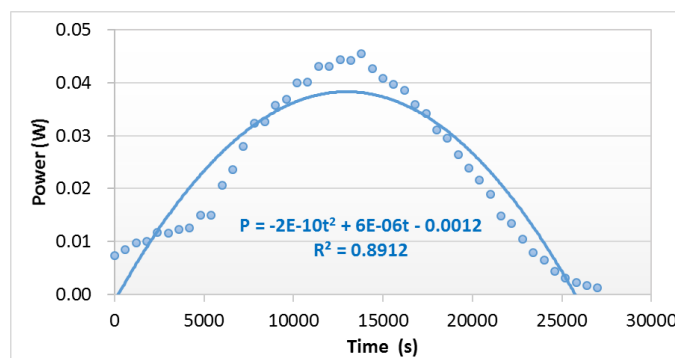


Fig. 11. Relationship between time and power of RTEGS.

The results show that, with the time increased, the powder of RTEGS increased first and then began to decline. And the relationship can be described by quadratic parabolic formula using the following equation.

$$P = -2E-10t^2 + 6E-06t - 0.0012 \quad (7)$$

Where t is the time (s).

The power output by the slab 300 mm \times 300 mm by size was about 840 J in 7.5 h by integral calculation using Eq. 7. To better understand the scale of power output, the energy generated by a road of 1 kilometer in length and 10 meter in width are calculated, which is about 9.36×10^7 J of energy, equivalent to 26 kilowatt-hour (kWh) of electricity in 7.5 h. And the output energy will be as high as 5.9×10^8 J in 8 h, equivalent to 160 kWh of electricity, if calculated using the data of road surface and ambient temperature measured on August 16th, 2016. The electric energy generated by the RTEGS can potentially be stored and used later, such as road lighting, traffic signal, communications, wireless monitoring system, and other electrical facilities by the roadside, or even charging facilities for electric vehicles in the future [40,41].

In order to understand the performance of the RTEGS, Table 1 lists some examples that represent the current road power generating technology [21,31,32,41].

Table 1
Parameters comparison for representative technology of energy harvesting from road

Technology	Company/researcher	Energy generation	Technology readiness levels (TRLs)
Photovoltaic	Solar Roadways	NA	4
	TNO	NA	7
Piezoelectric	Innowattech	5.8 J/vehicle	4
	Genziko	40 J/vehicle	4
TEG	Wu and Yu	2.6 mW/cm ³	3

Where NA represents Not Analyzed. TRLs are the measures used to evaluate the maturity of a technology during its developmental stages. These levels 1 to 9 were initially defined by the National Aeronautics and Space Administration (NASA) [21], but are now commonly used in project evaluations.

TRL 1 – basic principles observed and reported; TRL 2 – technology concept and/or application formulated; TRL 3 – analytical and experimental critical function and/or characteristic proof of concept; TRL 4 – component validation in laboratory environment; TRL 5 – component validation in relevant environment; TRL 6 –

system/subsystem model or prototype demonstration in a relevant environment; TRL 7 – system prototype demonstration in an operational environment; TRL 8 – actual system completed and qualified through tests and demonstration; TRL 9 – actual system proven in operational environment.

According to the calculation method used by Wu and Yu [31,32], the energy generation calculated was about 2.83 mW/cm^3 when output voltage of RTEGS was 0.7 V. The development stage of RTEGS was TRL 5 to TRL 6. Compared with the photoelectric conversion efficiency of 10% [21], the thermoelectric conversion efficiency of the road is still low, usually around 5%.

As mentioned, the testing site is in a temperate climate. Furthermore, due to buildings and trees nearby, the illumination time of the site was less than the available illumination time in the day. It is anticipated that for asphalt pavements in tropical and sub-tropical regions, more energy will be generated through the RTEGS. Field tests in those regions will help to quantify the actual outputs. In addition, the conversion efficiency of RTEG used in this test was only about 5% to 6% according to the manufacturer. With further development of the thermoelectric materials and technology, the output of RTEGS is likely to be enhanced, which will further promote the application of pavement thermoelectric technology for wider social and economic impacts.

7. Cost and environmental benefits

In terms of cost, the total cost of materials and production is 40 \$ for indoor test. The price of aluminum vapor chambers is about 10 \$, the price of TEG modules is 15 \$, and the cost of materials and production of the water tank is 15 \$. The costs for a road of 1 kilometer in length and 10 meter in width are estimated at about 90,000 \$ according to the cost of indoor test. Assuming the road service life of 15 years, and the price of electricity 0.2 \$ per kWh, when the annual average daily electricity generation is 100 kWh, 80 kWh and 60kwh, the income form

electric power generation can reach 108,000 \$, 86,400 \$ and 64,800 \$, respectively. This system is expected to be more profitable for tropical and subtropical regions where the radiation intensity and the average annual temperature is high. In addition, the materials' residual value at the end of road life was not taken into account in the above calculations. Furthermore, the cost of the system is expected to be further reduced when the scale of construction increases to industrial level.

Compared with the piezoelectric and photovoltaic road technology, thermoelectric road technology has significant environmental and social benefits. Fig. 12 displays the temperature collected outdoor of the traditional asphalt road surface and thermoelectric asphalt road surface on May 26th, 2017. It can be seen that the temperatures of thermoelectric asphalt road surface were much lower than that of traditional asphalt road under the natural sunlight, temperature and other environmental factors. The maximum temperature difference of traditional asphalt road surface and thermoelectric asphalt road surface was about 10 °C. The temperature difference exceeded 5 °C from 12:00 to 19:30. From the results above, thermoelectric asphalt road could significantly reduce the surface temperature of pavements and is currently considered a promising tool for alleviating urban heat island effect, as well as reducing defects of road associated with high temperature.

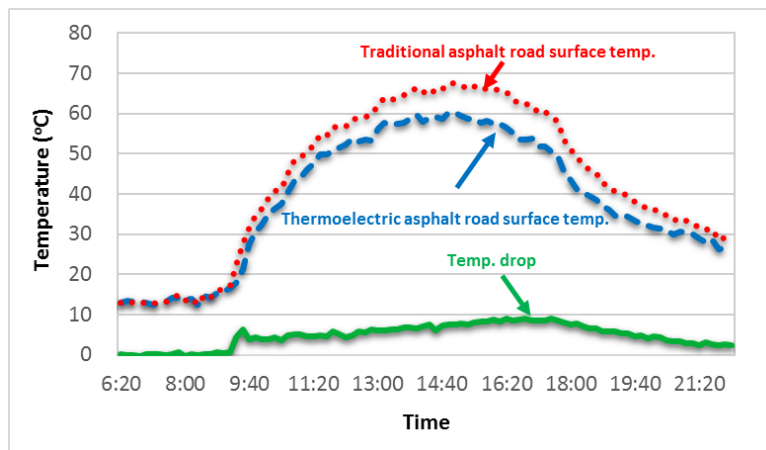


Fig. 12. Temperature data collected outdoor of the traditional asphalt road surface and thermoelectric asphalt road

surface. (May 26th, 2017)

This system can be further upgraded to reduce costs and enhance energy output, such as using municipal water supply pipeline instead of water tank fixed on the cold side of TEGs. In addition, it is also possible to consider connecting the TEGs cold side to one end of the vapor chamber, and the other end is buried at a certain depth in the ground for a relatively lower temperature. Practicality of these designs and the enhanced power output can be tested in further study to validate the above assumptions.

8. Conclusion and recommendations

In this paper, the road surface and ambient temperature characteristics was investigated. Studies for energy harvesting from asphalt pavement using thermoelectric technology were conducted and a road thermoelectric generator system was developed for electricity generation. From the indoor and outdoor test, the output voltage of developed RTEGS was tested, and regression analysis carried out to establish the relationship between energy output and temperature difference. The main work involved in this study, and results from the experiments are outlined below:

(1) A set of road thermoelectric generator system was developed. The heat was transferred out of the pavement by vapor chambers embedded in the pavement structure. The temperature difference between the road surface and ambient air, which produces electrical energy, was used to power the TEGs. A water tank was installed at the cold side of TEG to maintain a stable temperature difference. The system provides an innovative way for energy harvesting from asphalt pavement. Further studies are needed to prove the concept of embedding vapor chambers in pavement structure without compromising its mechanical performance and durability.

(2) The temperature difference between the road surface and ambient air, as well as the

temperature gradient within road structure, were gathered by a data acquisition instrument. The city of Xi'an, where the field tests were carried out, provides the necessary conditions for the application of thermoelectric technology. For asphalt pavement in tropical and subtropical regions, the larger temperature difference would be more suitable for RTEGS.

(3) Good linear correlations between output voltage and temperature difference were observed in the process of slab heating and cooling. That is, the output voltage increased linearly with the increase of temperature difference. However, due to the temperature gradients in pavement during the heating and cooling process, the intercepts of the regression line for indoor and outdoor tests were different. While the outdoor tests are more representative of the real road environment, indoor tests enable the control of environmental conditions to establish mathematical relationship between variables.

(4) When the temperature difference between road surface and ambient air is 15 °C in winter, the output voltage generated by RTEGS is about 0.4 V. Thus, the energy generated by a road of 1 kilometer in length and 10 meter in width is estimated to be $9.36 \times 10^7 \text{J}$ in 7.5 hours, equivalent to 26 kWh of electricity. While in summer, the output voltage generated is about 0.6 V to 0.7 V with 25 °C to 30 °C temperature difference, which means about 160kWh of energy can be obtained in 8 hours.

(5) In addition to harvesting energy from road, RTEGS can also reduce the road surface temperature which helps to alleviate the urban heat island effect as well as reduce pavement defects associated with high temperature. The maximum temperature difference of traditional asphalt road surface and thermoelectric asphalt road surface was about 10 °C. Therefore, the RTEGS has significant environmental and social benefits. A lifecycle cost-benefit analysis of the

RTEGS in pavement structure, considering the installation cost, income from energy generation as well as prolonged pavement life, will be very conducive to evaluate the cost implication of using the RTEGS.

(6) With the development of TEG materials and technology, the output energy of RTEGS and thus the efficiency of the system, is likely to be enhanced, which will further promote its application.

As a brand new technology, results from this study are quite encouraging. Further in-situ testing of the RTEGS in asphalt pavement is essential for optimizing the system, as well as evaluating the readiness for industrial use. In addition, it is recommended to consider the connection between the water tank of RTEGS and the water supply system around the road in a pilot scheme, which will improve the power generation efficiency of the system, as well as indicate any practical constraints of applying this technology.

Acknowledgements

This project was jointly supported by the National Natural Science Foundation of China (Grant No. 51608043), the Natural Science Basic Research Plan in Shaanxi Province of China (Grant No. 2015KJXX-23), the Fundamental Research Funds for the Central Universities (Grant No. 310821172001), and the Construction Science and Technology Plan in Shaanxi Province of China (Grant No. 2015-K99).

References

- [1] Webb J, Hawkey D, Tingey M. Governing cities for sustainable energy: The UK case. *Cities*, 2016, 54: 28-35.
- [2] Intergovernmental Panel on Climate Change (IPCC) (2014). Summary for policymakers. *Climate Change 2014: Impacts, Adaptation, and Vulnerability. Part A: Global and Sectoral Aspects* (pp. 1–32). Cambridge, United Kingdom and New York, NY, USA: Cambridge University Press.
- [3] Wang Z Y, Wennersten R, Sun Q. Outline of principles for building scenarios-Transition toward more sustainable energy systems. *Applied Energy*, 2017, 185: 1890-1898.

- [4] Yan J, Shamim T, Chou S K, Desideri U, Li H. Clean, efficient and affordable energy for a sustainable future. *Applied Energy*, 2017, 185: 953-962.
- [5] Dincer I, Acar C. Smart energy systems for a sustainable future. *Applied Energy*, 2016, <http://dx.doi.org/10.1016/j.apenergy.2016.08.088>. (In press).
- [6] Alper A, Oguz O. The role of renewable energy consumption in economic growth: Evidence from asymmetric causality. *Renewable and sustainable Energy Reviews*, 2016, 60: 953-959.
- [7] Khaligh A and Onar O C. *Energy Harvesting: Solar, Wind, and Ocean Energy Conversion Systems*. CRC Press Inc, Boca Raton, FL, USA, 2010.
- [8] Thomé A M T, Ceryno P S, Scavarda A, Remmen A. Sustainable infrastructure: A review and a research agenda. *Journal of Environmental Management*, 2016, 184: 143-156.
- [9] Andriopoulou S. A Review on Energy Harvesting from Roads. KTH, Stockholm, Sweden, 2012.
- [10] Moure A, Izquierdo Rodríguez M A, Hernández Rueda S, Gonzalo A, Rubio-Marcos F, Urquiza Cuadros D, Pérez-Lepe A, Fernández J F. Feasible integration in asphalt of piezoelectric cymbals for vibration energy harvesting. *Energy Conversion and Management*, 2016, 112: 246-253.
- [11] TNO. SolaRoad:paving the way to the roads of the future < <https://www.tno.nl/media/4574/solaroadtechnology.pdf>>; [Accessed February 6, 2017].
- [12] Dawson A, Mallick R, Hernandez A G, Dehdezi P K. *Energy Harvesting from Pavements*. Green Energy and Technology. Springer Press, 2014.
- [13] Tao J, Hu J. Energy harvesting from pavement via polyvinylidene fluoride: hybrid piezo-pyroelectric effects. *Journal of Zhejiang University-Science A (Applied Physics & Engineering)*, 2016, 17(7): 502-511.
- [14] Zhao H D, Tao Y J, Niu Y L, Ling J M. Harvesting energy from asphalt pavement by piezoelectric generator. *Journal of Wuhan University of Technology-Mater. Sci. Ed.* 2014, 10: 933-937.
- [15] Xiong H C, Wang L B, Wang D, Druta C. Piezoelectric energy harvesting from traffic induced deformation of pavements. *International Journal of Pavement Research and Technology*, 2012, 5(5): 333-337.
- [16] Xiong H C, Wang L B. Piezoelectric energy harvester for public roadway: On-site installation and evaluation. *Applied Energy*, 2016, 174: 101-107.
- [17] Kang-Won W and Correia A J. A Pilot Study for Investigation of Novel Methods to Harvest Solar Energy from Asphalt Pavements. Korea Institute of Construction Technology (KICT), Goyang City, South Korea, 2010.
- [18] Zhou Z, Wang X, Zhang X, Chen G, Zuo J, Pullen S. Effectiveness of pavement solar energy system – an experimental study. *Applied Energy*, 2015, 138: 1-10.
- [19] Roshani H, Dessouky S, Montoya A, Papagiannakis A T. Energy harvesting from asphalt pavement roadways vehicle-induced stresses: A feasibility study. *Applied Energy*, 2016, 182: 210-218.
- [20] Guldentops G, Nejad A M, Vuye C, Van den bergh W, Rahbar N. Performance of a pavement solar energy

- collector: model development and validation. *Applied Energy*, 2016, 63: 180-189.
- [21] Duarte F, Ferreira A. Energy harvesting on road pavements: state of the art. *Proceedings of the ICE-Energy*, 2016, 169: 79-90.
- [22] Motamed A, Bahia H U. Incorporating temperature into the constitutive equation for plastic deformation in asphalt binders. *Construction and Building Materials*, 2012, 29: 647-658.
- [23] Jiang W, Sha A, Xiao J, Li Y, Huang Y. Experimental study on filtration effect and mechanism of pavement runoff in permeable asphalt pavement. *Construction and Building Materials*, 2015, 100: 102-110.
- [24] Levinson R, Akvari H, Berdahl P, Wood K, Skilton W, Petersheim J. A novel technique for the production of cool colored concrete tile and asphalt shingle roofing products. *Solar Energy Materials & Solar Cells*, 2010, 94: 946-954.
- [25] Chen J Q, Wang H, Zhu H Z. Analytical approach for evaluating temperature field of thermal modified asphalt pavement and urban heat island effect. *Applied Thermal Engineering*, 2017, 113: 739-748.
- [26] Schreier M, Roschewsky N, Dobler E, Meyer S, Huebl H, Gross R, Goennenwein S T B. Current heating induced spin seebeck effect. *Applied Physics Letters*, 2013, 103(24): 1-5.
- [27] Snyder G J, Toberer E S. Complex Thermoelectric Materials. *Nature Materials*, 2008, 7:105-114.
- [28] Bell L E. Cooling, Heating, Generating Power, and Recovering Waste Heat with Thermoelectric Systems. *Science*, 2008, 321: 1457-1461.
- [29] Yavuzturk C, Ksaivati K, Chiasson A D. Assessment of temperature fluctuations in asphalt pavements due to thermal environmental conditions using a two-dimensional, transient finite difference approach. *Journal of Materials in Civil Engineering*, 2015, 17(4): 465-475.
- [30] Lee J J, Kim D H, Lee K H, L J K, Lee S T. Fundamental Study of Energy Harvesting using Thermoelectric Module on Road Facilities. *International Journal of Highway Engineering*, 2014, 16 (6): 51-57. (in Korean with English summary).
- [31] Wu G and Yu X. Thermal energy harvesting across pavement structures. *Proceedings of the Transportation Research Board (TRB) 91st Annual Meeting*. Transportation Research Board, Washington, DC, USA, 2012.
- [32] Wu G and Yu X. Computer-aided design of thermal energy harvesting system across pavement structure. *International Journal of Pavement Research and Technology*, 2013, 6 (2): 73-79.
- [33] Hasebe M, Kamikawa Y and Meiarashi S. Thermoelectric generators using solar thermal energy in heated road pavement. In *Proceedings ICT '06 – 25th International Conference on Thermoelectrics (ICT)*, Vienna, Austria. IEEE – Institute of Electrical and Electronics Engineers, New York, NY, USA, 2006: 697-700.
- [34] Guo L, Lu Q. Potentials of piezoelectric and thermoelectric technologies for harvesting energy from pavements. *Renewable and Sustainable Energy Reviews*. 2017, 72: 761–773.
- [35] Wu G, Yu X. A holistic 3D finite element simulation model for thermoelectric power generator element. *Energy Conversion and Management*, 2014, 86: 99–110.

- [36] Teltayev B, Aitbayev K. Modeling of temperature field in flexible pavement. *Indian Geotechnical Journal*, 2015, 45(4): 371-377.
- [37] Li Z S, Tan Y Q. Temperature field of asphalt pavement in seasonal frozen region suffered by freeze-thaw cycles. *Fourth International Conference on Transportation Engineering-ICTE*, 2013, 2122-2128.
- [38] Banks, D. *An Introduction to Thermogeology: Ground Source Heating & Cooling*”, Blackwell Publishing Ltd., Oxford, 2008.
- [39] Dawson A, Dehdezi P K, Hall M R, Wang J, Isola R. Enhancing thermal properties of asphalt materials for heat storage and transfer applications. *Road Materials and Pavement Design*, 2012,13 (4): 784-803.
- [40] Qiao G, Sun G, Li H, Ou J. Heterogeneous tiny energy: an appealing opportunity to power wireless sensor nodes in a corrosive environment. *Applied Energy*, 2014, 131: 87-96.
- [41] TNO. SolaRoad <https://www.tno.nl/media/2703/presentation-solaroad-definitief_uk.pdf>; 2011 [Accessed February 6, 2017].